

Malter effect in thin ITO films

JADWIGA OLESIK*, ZYGMUNT OLESIK

Institute of Physics, Jan Dlugosz University, al. Armii Krajowej 13/15, 42-201 Czestochowa, Poland

*Corresponding author: j.olesik@ajd.czest.pl

The subject of the study was field influence on electron emission into vacuum from ITO films deposited on glass surface. The films were deposited onto both surfaces of the glass and examined using the Malter effect controlled by electric field. One of the layers was the field electrode and the other was treated as the electron emitter. The bias voltage was applied to the field electrode. The analysis was carried out at a pressure of 10^{-5} Pa. Dependences of the secondary emission coefficient on the bias voltage and energy distributions of secondary electrons were determined. The diagrams obtained are characterized by high non-monotonic behaviour. The voltage pulse amplitude spectra were recorded in the multichannel amplitude analyzer. It has been found that pulses count depends exponentially on the bias voltage. The emission efficiency at the same inducing field is affected by the state in which the sample was before the measurement. This means that the field induced electron emission shows hysteresis-like behaviour. The existence of this effect proves that the electric field causes some irreversible changes in the electron emitting ITO layer.

Keywords: indium tin oxide (ITO), photon emission, field effect, electron emission.

1. Introduction

The phenomenon of enhanced secondary emission from a thin-film insulator on a metal base by the thin-film field emission effect was first reported by Louis Malter in 1936 [1]. He observed that secondary electron emission from the surface results in the establishment of a positive charge on the surface. This positive charge produces a high electric field, resulting in the emission of electrons through the surface. This tends to pull more electrons from further beneath the surface. Eventually, the sample replenishes lost electrons by picking up the collected secondary electrons through the ground loop.

Malter investigated secondary electron emission from a metal covered with a thin and poorly conducting film ($\text{Al}-\text{Al}_2\text{O}_3-\text{Cs}_2\text{O}$). Oxidized films possess new and interesting properties when subjected to electron bombardment in the presence of an adjacent collector electrode, whose potential is held positive with respect to the aluminium. True secondary electron emission from treated surface results in the establishment of

a positive charge on the surface and polarization of the oxide film. This positive charge acting through the thin oxide film produces a high gradient electric field, resulting in the emission of electrons through the surface. The emission increases with collector voltage and beam currents, obeying power laws, but exhibits saturation tendencies. The removal of the primary beam does not result in the immediate cessation of the field emission, but rather in a slow decay which is due to the fact that the surface charge takes an appreciable time to leak away [1, 2].

It has been observed that when the primary beam was switched off, the emission current persisted for many hours. This effect was interpreted as follows: the positive charges, which were formed at the surface of the insulator due to the secondary electron emission indicating the yield larger than unity, produce a field large enough to cause field emission from the metal base. When voltage above a certain threshold is applied across a metal–insulator–metal thin-film sandwich, high currents exist; if the anode side of the metal film is thin enough, high electron emission into the vacuum is observed. The field, once it has been established, remains for an extended period due to the slow process of charge neutralization and high resistivity. This effect has been rediscovered recently by workers in the semiconductor device field [3–5].

Based on Malter's results, control of the secondary emission by the generation of an inner electric field in a sample is an interesting possibility. The glasses covered on both sides with thin conducting films were used as samples. This form of samples enabled the internal field to be controlled by the bias voltage. It is easy to determine the electric field intensity inside the glass, but it is much more difficult to determine its value in the emitting film; particularly when it is bombarded by primary electrons. The U_{bias} voltage applied to the sample generates circumstances similar to those observed in Malter effect. It results in the occurrence of certain effects accompanying electron emission phenomenon, which are the subject of this paper. The interest in thin films such as SnO_2 , In_2O_3 , ZnO , Cd_2SnO_4 , CdIn_2O_4 , known as TCO (transparent conducting oxide) films in technological applications is the result of their high infrared reflectance, high luminous transmittance and good electrical properties [6, 7].

2. Apparatus and samples

In the analysis, a rectangular-shaped sample of a microscopic cover glass ($20 \times 20 \times 0.2$ mm) with $\text{In}_2\text{O}_3:\text{Sn}$ (ITO) layers deposited on both sides was used. One film was an emitter of electrons and the other was a field electrode (Fig. 1). The films were deposited by dc reactive sputtering in the $\text{Ar} + \text{O}_2$ atmosphere [8, 9]. The sputtered target was an alloy of 90% In + 10% Sn. The total pressure was 6 Pa and the discharge voltage was 2 kV. The thickness of the front film varied within the range of 100–200 nm. The field electrode was 1 μm thick. The film thickness was measured by a Talysurf 4 profilometer [8]. The resistance of the films was measured using four-electrode method (from 8×10^{-4} to 3×10^{-3} Ωcm) [10, 11]. The sheet

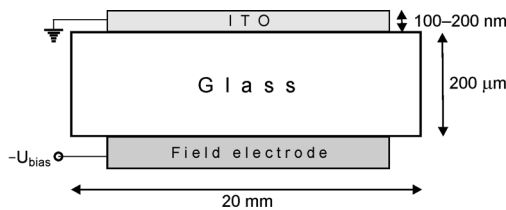


Fig. 1. Shape and size of a sample.

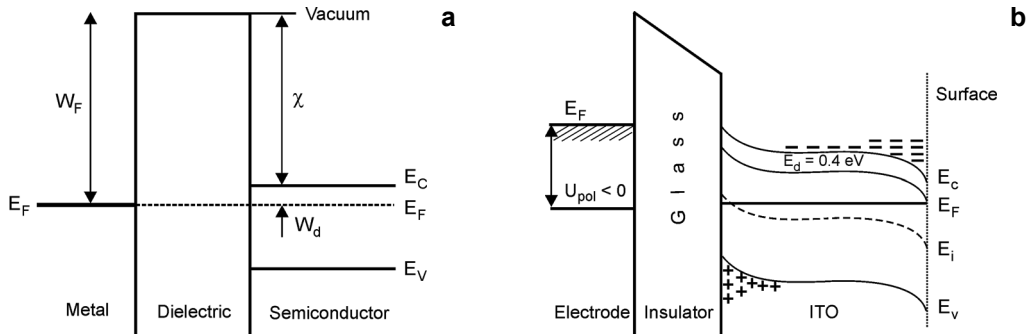


Fig. 2. Energy band diagrams of glass–ITO system for: ideal structure without bias (a), and structure with bias (b). E_c – the bottom of the conduction band, E_v – the top of the fundamental band, E_F – Fermi level, E_d – donor level, W_F – work function for field electrode, W_d – flat band work function, χ – electron affinity, U_{bias} – biasing voltage.

resistance varied within 10–100 Ω/sq . The film composition studied by X-ray electron microprobe analysis was found to be almost independent of the sputtering. The doped ITO layers appear to be wide gap n -type polycrystalline semiconductors, the conductivity of which depends among others on doping concentration. The forbidden gap was found to be 3.5 to 4 eV wide. At concentration of about 10^{25} m^{-3} the donor levels split and the semiconductor becomes degenerated. The ITO layers on the glass substrate can be assumed to be degenerated if they are sufficiently thick, so the substrate influence can be neglected. A band model of emitter system is presented in Fig. 2 [12, 13]. The remaining electrical and optical properties of ITO layers are given in papers [11, 14–16]. By applying an appropriate voltage to the layers one may create an inner electric field of a given direction and value. The field electrode was characterized by great transmittance, which enabled us to study the transmission photoemission of electrons. Optical transmission of the films was measured using a double-beam spectrophotometer and equalled about 90% in the visible range of the light spectrum [16, 17]. The sample was placed in the vacuum of 10^{-5} Pa .

The internal electric field in the sample was generated by high voltage power supply, which allowed a negative biasing voltage to be applied to the bottom electrode of the sample. A scheme of the electric set used to study the field induced secondary emission (FISE) is presented in Fig. 3a. The energy of the primary electron beam was

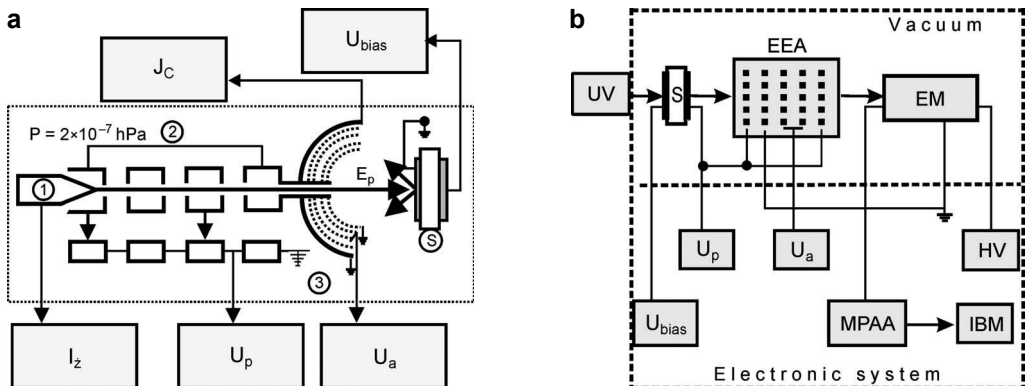


Fig. 3. Experimental setup used to study the field induced secondary emission (FISE) – a, and the field induced electron emission (FIEE) – b. 1 – electron gun CL-305, 2 – accelerating system, 3 – four-grid retarding potential analyzer, S – sample, U_p – accelerating voltage, U_a – analyzing voltage, J_c – collector voltage, U_{bias} – biasing voltage, E_p – primary electron energy, UV – quartz lamp, EEA – energy electron analyzer, EM – electron multiplier (channeltron), HV – high voltage switch, (2.9 kV), MPAA – multichannel pulse amplitude analyzer, IBM – computer.

changed from 25 eV to 200 eV. Secondary electrons from the sample were directed to the electron energy analyzer. A four-grid retarding potential analyzer makes it possible to investigate change in the secondary emission coefficient when all the grids are short circuited and grounded. To obtain the electron energy distribution, the negative potential U_a is applied to the analyzing grids. U_a potential is negative in relation to the emitting surface of the sample.

In order to minimise the Malter effect and accompanying it charging of the sample surface as a result of primary electron bombarding, it was decided to investigate only field induced electron emission, *i.e.*, without participation of primary beam. A schematic diagram of the apparatus used to study the field induced electron emission (FIEE) is shown in Fig. 3b. Applying the biasing voltage U_{bias} , from the interval from -2 kV to 0 V to the field electrode creates an internal field, which favours electron emission into vacuum. Appropriate operational conditions for the electron multiplier were obtained by acceleration of electrons between the emitting film and the multiplier, *i.e.*, voltage $U_p = -200$ V at the emitting film and grounded entrance of the multiplier (EM). Depending on the kind of measurements performed, grids 3 and 4 of the electron energy analyzer (EEA) were either grounded or polarized by the negative analyzing voltage U_a . The electrons accelerated to the energy eU_p create voltage pulses in the multiplier. These pulses are recorded in the multichannel pulse amplitude analyzer (MPAA). The multiplier is connected to preamplifier, which adjusts its parameters to MPAA. The multichannel analyzer registers pulses which are amplified. The pulses are recorded according to their height, creating the so-called voltage pulse amplitude spectrum. The amplitude spectra (for various U_{bias}) were measured for unilluminated samples and samples illuminated by a quartz lamp (UV).

3. Results

The collector current depending on U_{bias} voltage was determined using the apparatus shown in Fig. 3a. The secondary electron emission coefficient δ was determined from the dependence $\delta/\delta_0 = J_C/J_{C0}$, where: J_C is the collector current for $U_{\text{bias}} \neq 0$, J_{C0} is the collector current for $U_{\text{bias}} = 0$, and δ_0 is coefficient for $U_{\text{bias}} \neq 0$. The value of δ_0 was determined by measuring current in the sample and primary beam current using a Faraday cup. In this way, from the experimental dependence $J_C = f(U_{\text{bias}})$ the dependence $\delta = f(U_{\text{bias}})$ was obtained. Figure 4 shows $\delta = f(U_{\text{bias}})$ curves for samples with 20 nm thick ITO film. It is noticeable that when U_{bias} voltage rises, the coefficient δ decreases at first and then reaches its maximum levels. Further increase of U_{bias} voltage causes the coefficient δ to disappear. Values of U_{bias} voltage, at which coefficient δ reaches its minimum and maximum levels depend on energy E_p and that is why with the growth of energy E_p , $\delta(U_{\text{bias}})$ curve shifts in the direction of negative U_{bias} voltages.

The energy distributions of secondary electrons were measured for samples with various ITO film thicknesses, at various biasing voltages U_{bias} and energies E_p . Figure 5 shows $F(E)$ distributions for values of U_{bias} corresponding to characteristic changes in the coefficient δ shown in Fig. 4 (curve for $E_p = 100$ eV). The measurements of energy distributions were performed on the same sample just after measurement of coefficient δ dependence on field intensity. At $U_{\text{bias}} = 0$ the energy spectra are typical of semiconductors. In the interval of U_{bias} corresponding to the minimum of $\delta(U_{\text{bias}})$ decay of the $F(E)$ function is observed. In the interval of U_{bias} corresponding to the maximum I of $\delta(U_{\text{bias}})$ a shift in the primary peak in the lower energy direction is observed. In the region of maximum II of $\delta(U_{\text{bias}})$ secondary electrons of energy larger than the primary energy E_p are detected.

After eliminating the primary electron beam, FIEE was investigated using the apparatus shown in Fig. 3b. There were noticed certain anomalies concerning

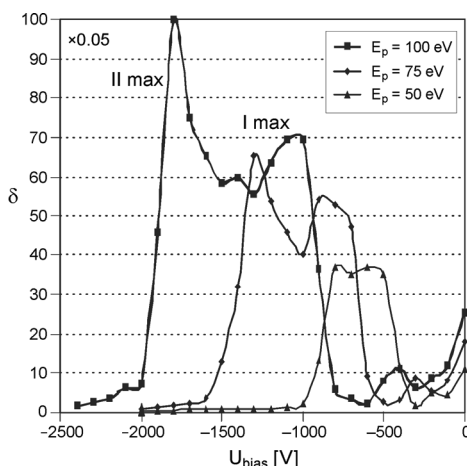


Fig. 4. Dependences of the coefficient δ on U_{bias} for a 20 nm thick ITO film.

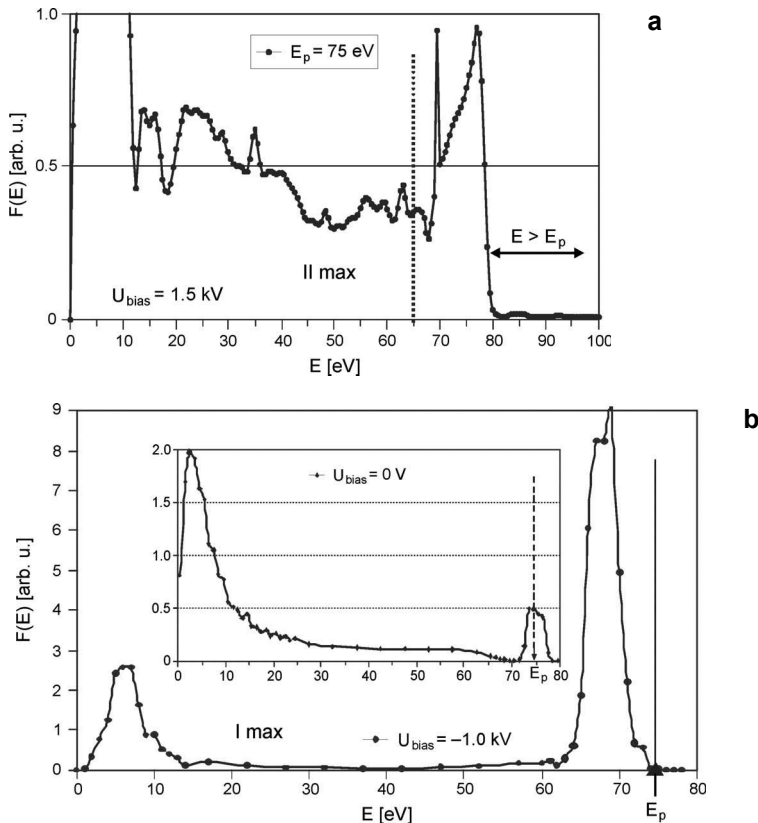


Fig. 5. Energy spectrum of secondary electrons for $U_{\text{bias}} = 1.5 \text{ kV}$ (II max of $\delta(U_{\text{bias}})$) – a. Energy spectra of secondary electrons for $U_{\text{bias}} = 0$ and $U_{\text{bias}} = 1 \text{ kV}$ (I max of $\delta(U_{\text{bias}})$) – b.

the course of this phenomenon. They can be connected with Malter effect. In order to prove this, the investigation was conducted in such a way that: in one case the measurements were performed for the applied voltage changing from 0 V to -2 kV and in the second case in the reverse direction, from -2 kV to 0 V. The multichannel pulse analyzer recorded the amplitude spectra of voltage pulses, which were created by electrons entering the multiplier. The number of pulses with amplitudes within a certain interval around the mean value appears to be proportional to the number of electrons emitted from the sample. Examples of spectra for selected U_{bias} are given in Fig. 6. The two spectra were found to be different for the same U_{bias} . They differed by the total number of pulses as well as by the mean amplitude connected with the mean energy of the emitted electrons. When U_{bias} changes in the reduction direction, the total number of pulses is always found to be larger than in the rise direction. The shift effect has also been found during the repeated measurement of the spectra at the same applied voltage. The pulse frequency n , which is the number of pulses recorded during 1 s, can be measured and the dependence of frequency n on the voltage U_{bias} is presented in Figs. 7 and 8. These curves successfully illustrate the influence

of the voltage U_{bias} on electron emission intensity for ITO films without UV illumination as well as under illumination.

The above results lead to the conclusion that the FIEE from ITO layers shows a hysteresis effect. This results from the fact that the emission phenomena were found to be different depending on whether U_{bias} voltage is increasing or decreasing during

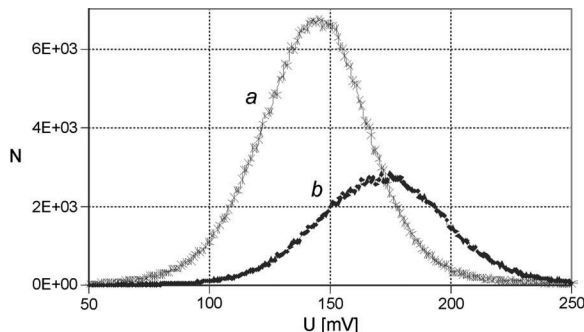


Fig. 6. Pulse amplitude spectra for $U_{\text{bias}} = -2 \text{ kV}$. Curve *a* – variation of U_{bias} in direction from -2 kV to zero, curve *b* – variation of U_{bias} in direction from zero to -2 kV .

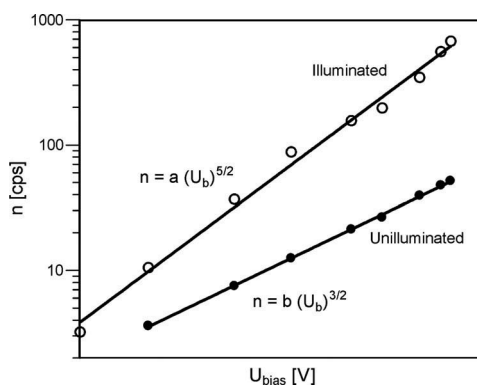


Fig. 7. Frequency count as a function of biasing voltage for 200 nm thick ITO film; $a = 2 \times 10^{-4}$, $b = 5 \times 10^{-4}$.

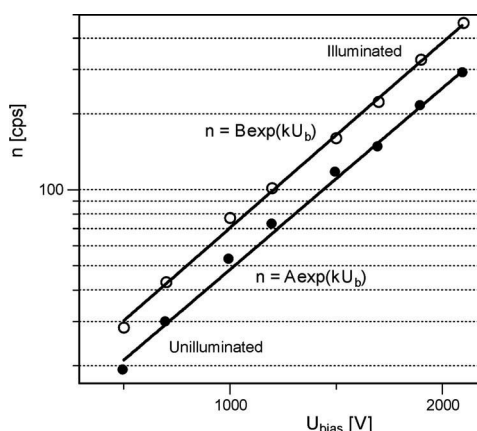


Fig. 8. Frequency count as a function of biasing voltage U_{bias} for 100 nm thick ITO film; $A = 10$, $B = 15$, $k = 2 \times 10^{-3}$.

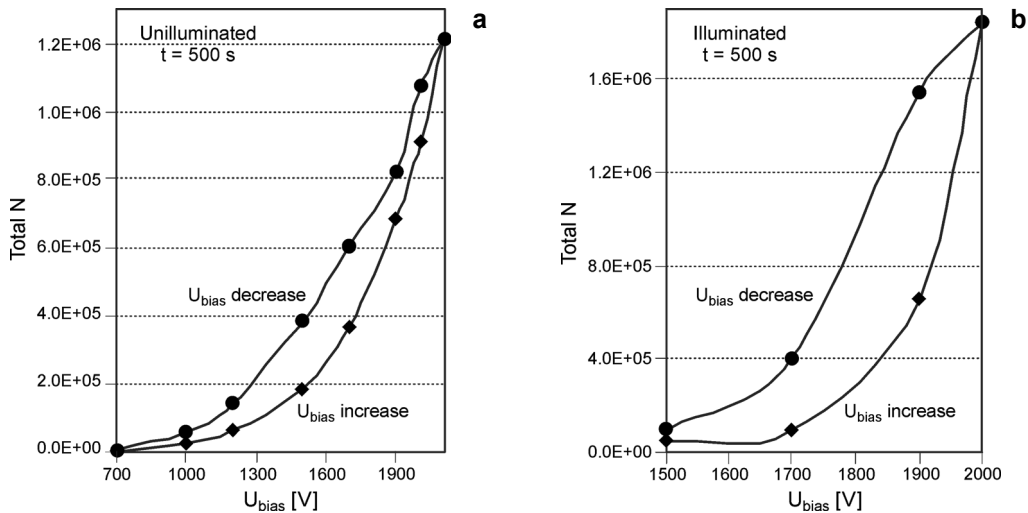


Fig. 9. The photoelectro-emission hysteresis: ΣN as a function of voltage U_{bias} . Increase – variation of U_{bias} in the direction from zero to $-U_{\text{bias}}$, decrease – variation of U_{bias} in the direction from $-U_{\text{bias}}$ to zero.

the measurement process. This means that under the same electric field inducing emission (the other parameters being the same) the emission efficiency is different depending on the field variation direction, *i.e.*, the growing or reducing of the field. In order to examine the effect, the total number of counts ΣN as a function of voltage U_{bias} has been measured for different U_{bias} voltage and different directions of its variation. The diagrams $\Sigma N = f(U_{\text{bias}})$ have been drawn for both series of measurements. Figure 9 shows the dependences ΣN as a function of voltage U_{bias} for the applied voltage changed from 0 V to -2 kV and in the second case in the reverse direction.

4. Discussion

When the difference of work functions between the system elements (a capacitor-like structure) is neglected, then the applied voltage U_{bias} is distributed between glass (U_g) and semiconductor (U_I): $U_{\text{bias}} = U_g + U_I$, where $U_g = Q/C_g$ and $U_I = Q/C_I$. If we assume that the band of the semiconductor is flat, as in Fig. 2, then capacitance C_g and C_I per surface unit [F/m^2] can be appropriately presented as: $C_g = \epsilon_0 \epsilon_g / d$, $C_I = \epsilon_0 \epsilon_I / L_D$, where L_D – Debye shielding length, d – glass thickness. Capacitance C_I is related to the region with space charge in the ITO semiconductor. The value of C_I depends on the depleted region width in the semiconductor layer, *i.e.*, on the value of voltage U_{bias} . The total system capacitance is a series connection of C_g and C_I capacitances. Assuming $d = 2 \times 10^{-4}$ m, $L_D \leq 2 \times 10^{-7}$ m (ITO thickness), $\epsilon_g \approx 10$ and $\epsilon_I < \epsilon_g$, one can determine the dependence between the voltage distribution on the dielectric and on the semiconductor layer: $C_g = 2 \times 10^{-3} C_I$ and $U_I = 2 \times 10^{-3} U_g$.

Taking this into account, one can estimate the electric field value in glass and in ITO layer (for instance, for $U_{\text{bias}} = 1 \text{ kV}$: $U_g = 998 \text{ V}$, $U_I = 2 \text{ V}$):

$$E_g = \frac{U_g}{d} \approx 5 \times 10^6 \quad \left[\frac{\text{V}}{\text{m}} \right]$$

$$E_I = \frac{U_I}{L_D} \approx 10^7 \quad \left[\frac{\text{V}}{\text{m}} \right]$$

When a semiconductor is under influence of the external electric field, the free charge carriers are forced to change their spatial distribution (Fig. 2). Initially, at a moderate voltage U_{bias} applied, a relatively homogeneous polarization in the entire volume of semiconductor occurs without formation of enhancement and depletion regions. The energy gained by electrons as a result of these fields is not larger than about kT , that is why the electrons cannot be emitted into vacuum. The energy of electrons accelerated in the field can be larger than the value of thermal energy, so $E > kT$, when the field increases. This additional energy can appear to be sufficient for hot electrons to be able to surmount the surface potential barrier [18, 19]. At high voltages of U_{bias} (more than 1 kV) conditions created in the semiconductor correspond to $E \gg kT$. This means that in the ITO layer two separate regions are created: depletion at the glass surface and enhancement at the vacuum boundary. The field intensity at this region of ITO is of the order of 10^7 V/m . With an increase of the field intensity the enhancement layer is narrowed, thus electron concentration is higher [20].

In the depleted region, the field has direct effect upon electron concentration in the conduction band of ITO and in the enhanced zone the field action seems to be partly screened, so the field does not affect directly the electron concentration. The shift of the elastic peak in the energy spectrum to energies lower than E_p can be related to the reduction in the number of elastically reflected electrons from the emitter surface (Fig. 6). This means that the majority of the electrons are subjected to the energy reduction (below E_p) and this occurs at the surface zone of ITO. With increasing U_{bias} voltage the number of electrons penetrating the enhanced zone of ITO rises, but only part of them are able to go outside the film. This results in a dynamic widening of the enhanced zone. So, if we apply the field once again, we do not obtain the same conditions in the emitting layer. Carrier concentration as well as the enhanced layer width appear to be changed [21]. At a certain value of U_{bias} the enhanced zone may be so thin that some electrons penetrate into the depleted zone without energy loss. The transparency of the enhanced zone may be related to the possibility of multiple electron collisions in the depleted zone leading to the energy gain greater than E_p [22]. The probability of such collisions is very small however. The occurrence of maximum II on the $\delta(U_{\text{bias}})$ curve and the observation of high energy secondary electrons could possibly be explained by this effect.

On the other hand, the possibility of electron emission into vacuum can be described by certain mechanisms mainly based on the bulk structural defects. In

the ITO materials the main defects are oxygen vacancies and internodal ions of the admixtures [23, 24]. The top voids, pores or bulk vacancies can be a source of high local electric fields. These fields can produce avalanche multiplication of the electron stream. The normal emission takes place if electrons from the conduction band achieve energies higher than the mean thermal energy (kT). The electron can be emitted from the material if this excess of energy is higher than the work function (lowered by field). When a defect is present on a surface, then the field geometry is disturbed and electrons can be easily extracted by the local fields ($F > 10^7$ V/m). These effects dominate at mean values of fields. The similar role is played by the defects localised in the glass–ITO interface. Single defects in the electric field such as oxygen vacancies can form clusters leading to defect channels [25, 26]. The channel can be imagined as a space where electron can be accelerated without a loss of energy.

The hysteresis effects are connected with the lack of stability, which is due to the fluctuations of the electric field in the surface layer as well as in the glass–ITO interface. The fluctuations occur as a result of creation of a domain structure that diminishes very slowly. The existence of the hysteresis proves that the electric field causes some irreversible changes in the emitting ITO layer. Usually the variation in electron emission is connected with the occurrence of additional charge at the surface of emitting sample or with the effect of self-supporting emission like in the case of the Malter emission. It is possible that electrons enter the surface layer of ITO, where their concentration is high (accumulation effect by the applied voltage). Electrons in order to escape into vacuum suffer the loss in energy due to the larger amount of collisions with other electrons and atoms. As a result the emitted electrons show reduced mean energy. These effects occur because the dielectric and semiconducting film is, or becomes, an electrically nanostructured heterogeneous material [24, 27].

5. Conclusions

In the paper, we have studied FISE and FIEE phenomena in capacitor-like structures with thin ITO layers on the glass substrate. ITO films were from 100 to 200 nm in thickness and the value of field intensity varied from 1 to 10 MV/m which corresponds to the bias voltage of the range from –200 to –2000 V. This electric field can create defects, pores and lossless channels, the dimensions of which are of the nanometer range [24]. Local field in ITO layer is larger than 10^7 V/m.

During the research several interesting effects have been observed. These effects can be explained by phenomenological model of ITO layer division into two regions with depleted and enhanced number of electrons:

- $\delta(U_{\text{bias}})$ curves are non-monotonic,
- the yields of electron emission depend on the applied bias voltage and rise exponentially with an increase in U_{bias} ,
- energy spectra of secondary electrons show some field modifications depending on the U_{bias} value,

- there were detected secondary electrons with energy larger than the primary energy E_p ,
- photoelectron-emission hysteresis phenomenon related to the Malter effect was observed.

Studies conducted in this paper can be used in research and application of thin ITO films to production of channel electron multipliers. Malter effect can be applied in constructing multipliers of high effectiveness; however, it is essential to ensure stability of their functioning by controlling electric field intensity in emitting surface. We believe that the glass–ITO system might find application as voltage-controllable emitting photocathodes.

References

- [1] MALTER L., *Thin film field emisson*, Physical Review **50**(1), 1936, pp. 48–58.
- [2] KOLLER L.R., JOHNSON R.P., *Visual observations on the Malter effect*, Physical Review **52**(5), 1937, pp. 519–523.
- [3] JEONGHEE LEE, TAEWON JEONG, SEGI YU, SUNGHWAN JIN, JUNGNA HEO, WHIKUN YI, KIM J.M., *Secondary electron emission of MgO thin layers prepared by the spin coating method*, Journal of Vacuum Science and Technology B **19**(4), 2001, pp. 1366–1369.
- [4] KISELYOV V.K., KULESHOV E.M., LAPTIY V.K., *Research of terahertz-band gas HCN laser with the Malter effect in hollow cathode*, Telecommunications and Radio Engineering **63**(7–12), 2005, pp. 913–923.
- [5] HUA QIN, HYUN-SEOK KIM, BLICK R.H., WESTPHALL M.S., SMITH L.M., *Subthreshold field emission from thin silicon membranes*, Applied Physics Letters **91**(18), 2007, p. 183506.
- [6] WEIJTENS C.H.L., VAN LOON P.A.C., *Low resistive, ohmic contacts to indium tin oxide*, Journal of the Electrochemical Society **137**(12), 1990, pp. 3928–3930.
- [7] KHALID A.H., REZAZADEH A.A., *Fabrication and characterisation of transparent-gate field effect transistors using indium tin oxide*, IEE Proceedings: Optoelectronics **143**(1), 1996, pp. 7–11.
- [8] ZAKRZEWSKA K., LEJA E., *The electrical and optical properties of CdIn₂O₄ thin films prepared by dc reactive sputtering*, Vacuum **36**(7–9), 1986, pp. 485–487.
- [9] LEJA E., STAPIŃSKI T., MARSZALEK K., *Electrical and optical properties of conducting N-type Cd₂SnO₄ thin films*, Thin Solid Films **125**(1–2), 1985, pp. 119–122.
- [10] GRANQVIST C.G., HULTAKER A., *Transparent and conducting ITO films: new developments and applications*, Thin Solid Films **411**(1), 2002, pp. 1–5.
- [11] MAY C., STRUMPFEL J., *ITO coating by reactive magnetron sputtering—comparison of properties from DC and MF processing*, Thin Solid Films **351**(1–2), 1999, pp. 48–52.
- [12] VUL' A.YA., DIDEIKIN A., *Photodetectors based on metal-tunnel insulator-semiconductor structures*, Sensors and Actuators A: Physical **39**(1), 1993, pp. 7–18.
- [13] PRZEWLOCKI H.M., *Photoelectric phenomena in metal-insulator-semiconductor structures at low electric fields in the insulator*, Journal of Applied Physics **78**(4), 1995, pp. 2550–2557.
- [14] ORITA M., TANJI H., MIZUNO M., ADACHI H., TANAKA I., *Mechanism of electrical conductivity of transparent InGaZnO₄*, Physical Review B **61**(3), 2000, pp. 1811–1816.
- [15] EDERTH J., JOHNSSON P., NIKLASSON G.A., HOEL A., HULTAKER A., HESZLER P., GRANQVIST C.G., VAN DOORN A.R., JONGERIUS M.J., BURGARD D., *Electrical and optical properties of thin films consisting of tin-doped indium oxide nanoparticles*, Physical Review B **68**(15), 2003, p. 155410.
- [16] BOYCHEVA S., KRASILNIKOVA SYTCHKHOVA A., PIEGARI A., *Optical and electrical characterization of r.f. sputtered ITO films developed as art protection coatings*, Thin Solid Films **515**(24), 2007, pp. 8474–8478.

- [17] GROSS M., WINNACKER A., WELLMANN P.J., *Electrical, optical and morphological properties of nanoparticle indium-tin-oxide layers*, Thin Solid Films **515**(24), 2007, pp. 8567–8572.
- [18] FITTING H.-J., MÜLLER G.O., MACH R., REINSPERGER G.U., HINGST TH., SCHREIBER E., *Vacuum emission of hot electrons from ZnS*, Physica Status Solidi (a) **121**(1), 1990, pp. 305–313.
- [19] FITTING H.-J., SCHREIBER E., HINGST TH., *Avalanche measurement in ZnS by vacuum emission*, Physica Status Solidi (a) **122**(2), 1990, pp. K165–K168.
- [20] OLESIK J., *Influence of an internal electric field in a sample on the photoemission phenomenon*, Thin Solid Films **346**(1–2), 1999, pp. 191–195.
- [21] OLESIK J., CAŁUSIŃSKI B., *Influence of an internal electric field in a sample on the secondary electron emission phenomenon*, Thin Solid Films **238**(2), 1994, pp. 271–275.
- [22] IBACH H., *Surface vibrations of silicon detected by low-energy electron spectroscopy*, Physical Review Letters **27**(5), 1971, pp. 253–256.
- [23] SHABBIR A. BASHAR, *Study of Indium Tin Oxide (ITO) for Novel Optoelectronic Devices*, Ph.D. Thesis, Department of Electronic Engineering, University of London, 1998.
- [24] FITTING H.-J., HINGST TH., SCHREIBER E., *Breakdown and high-energy electron vacuum emission of MIS-structures*, Journal of Physics D: Applied Physics **32**(16), 1999, pp. 1963–1970.
- [25] EDERTH J., HULTAKER A., NIKLASSON G.A., HESZLER P., VAN DOORN A.R., JONGERIUS M.J., BURGARD D., GRANQVIST C.G., *Thin porous indium tin oxide nanoparticle films: effects of annealing in vacuum and air*, Applied Physics A: Materials Science and Processing **81**(7), 2005, pp. 1363–1368.
- [26] EDERTH J., HESZLER P., HULTAKER A., NIKLASSON G.A., GRANQVIST C.G., *Indium tin oxide films made from nanoparticles: models for the optical and electrical properties*, Thin Solid Films **445**(4), 2003, pp. 199–206.
- [27] EDERTH J., NIKLASSON G.A., HULTAKER A., HESZLER P., GRANQVIST C.G., VAN DOORN A.R., JONGERIUS M.J., BURGARD D., *Characterization of porous indium tin oxide thin films using effective medium theory*, Journal of Applied Physics **93**(2), 2003, pp. 984–988.

Received June 19, 2009
in revised form July 31, 2009